# Dynamics of low and high density microplastics in the world´s largest choked coastal lagoon under contrasting meteoceanographic conditions

Kristhal Doto[a*], Pablo Silva[a], Rémi Bouyssou[b], Isabel Jálon-Rojas[c], Elisa Helena Fernandes[a]

[a] Universidade Federal do Rio Grande (FURG), Lab. Oceanografia Costeira e Estuarina (LOCOSTE), Brazil

[b] INRAE Nouvelle-Aquitaine Bordeaux, France[c] CNRS, Bordeaux INP, EPOC Laboratory, Pessac, France

*Corresponding author

Email address: kristhaldotto@gmail.com

Postal address: Av. Itália km 8, Rio Grande (RS), 96203-900 BRASIL

## ABSTRACT

The contamination by plastic waste in aquatic environments has become a global issue, scientifically reported since 1970. The size and durability of microplastics (MPs, 1 µm > 5 mm) have made these debris widely distributed in aquatic environments. Despite various ongoing initiatives, there is a need to fill gaps in understanding how MPs are transported from their release sources to their final destinations. Therefore, understanding the distribution and dynamics of MPs in coastal areas, such as lagoons and estuaries, which are considered continental sources of MPs to the oceans, is essential to help fill these gaps and propose alternatives for managing what is the environmental problem of the century. In this context, this study aimed to assess the transport patterns of MPs in Patos Lagoon, the largest choked coastal lagoon in the world, considering contrasting meteoceanographic conditions in the system dynamics, such as wind and discharge. Using the hydrodynamic model TELEMAC-3D and the model for plastics particles TrackMPD, simulations were performed using a type of MP polymer (Polypropylene - PP). The simulations of MP transport considered advection, dispersion and the contribution of biofilm in increasing particle density (representing high-density microplastics). The results indicated a gradient of MPs retention from north to south, with higher concentrations of MPs occurring in the northern part of the system. The central region of the lagoon showed a greater tendency for MP export towards the southern region than retention. Meanwhile, the estuary region of Patos Lagoon exhibited a tendency for export of low-density MPs free of biofilm and retention of higher-density MPs, subject to the action of the Plastisphere. Additionally, based on the results obtained from density occurrence maps, it was possible to suggest potential accumulation areas of MPs throughout the lagoon system, reinforcing that the system can act as a sink in specific regions.

Keywords: plastic contamination; plastic accumulation; hot spots; estuaries; coastal lagoons; numerical modelling.

## 1. INTRODUCTION

The presence of plastic debris in aquatic environments has been documented in the scientific literature since the early 1970s, and in contemporary times, plastic contamination became ubiquity in these environments. The origin of plastics in the oceans can be attributed to both continental and maritime sources. According to Andrady (2011), approximately 80% of this contribution is linked to microplastics from continental sources (Li et al., 2018), which are highly susceptible to enter the aquatic environment through rivers, surface runoff, and wastewater systems because of their low density and weight (Horton et al. 2017). Meijer et al. (2021) estimated that between 0.08 and 2.7 million tons of plastics enter the oceans annually through rivers.

Among the different aspects related to the problem, special attention can be given to microplastics (MPs), which encompasses a diverse array of microparticles and fibers, typically ranging in size from 1 μm to 5 mm (Hanvey et al., 2017). Unlike their larger plastic counterparts, MPs may be of primary origin, intentionally manufactured in this size range (as pellets), or of secondary origin, resulting from the gradual breakdown of larger plastic items within the environment (Horton et al., 2017). Their small size and enduring nature present distinct challenges, as they can easily infiltrate and persist within marine and coastal ecosystems indefinitely. From surface waters to the ocean floor, microplastics have been documented (Barnes et al., 2009; Ling et al., 2017, Pan et al., 2019; Abel et al., 2021; Erkan et al., 2023; Tsuchiya et al., 2024), directly and indirectly affecting these environments. Their presence give rise to detrimental consequences, including alterations in habitats (Gall & Thompson, 2015), disruptions to socio-economic activities, adverse effects on aquatic organisms (Wright et al., 2013; Koelmans et al., 2016), and even potential implications for human health (Napper et al., 2019).

Despite various initiatives to understand the transport and distribution patterns of MPs in different aquatic compartments, obtaining a comprehensive global view of their distribution remains challenging. Discrepancies between the estimated amount of plastic floating on the ocean surface (Eriksen et al., 2014) and the estimated amount entering the ocean (Jambeck et al., 2015) suggest that some of this debris may be retained near its source regions. With approximately half of the world's population living within 80 km of the coast, coastal areas are already indicated as sources of plastics to the oceans (Cole et al., 2011) as well as accumulation environments (sinks). High concentrations have been observed in port areas (Auta et al., 2017), as well as salt marshes (Weinstein et al., 2016; Pinheiro et al., 2021) and estuaries (Díez-Minguito et al., 2020; Forero-López et al., 2021; Shabaka et al., 2022; Banik et al., 2024).

The distribution of these debris can be complex, with a significant portion remaining suspended in the water column (Ikenoue et al., 2023), while some may sink (Lobelle et al., 2021), and others may be transported to beaches (Ranjani et al., 2022) and coastal areas. Generally, microplastics with a density range lower (higher) than the surrounding fluid are more likely to float (sink) in the water column (Waldschläger & Schüttrumpf, 2019), being considered low-density (high-density) MPs. Low-density MPs, such as polypropylene, have a density range of 0.90-0.99 g/cm$^3$; however, particle density may vary due to biofouling development (Chubarenko et al., 2016), resulting in high-density MPs. Among the processes that can be responsible for the removal of MPs from the surface, one of the most relevant is biofouling (Kaiser et al., 2017). This can be defined as the colonization of micro to macro-organisms on the surface of a consolidated substrate, and it is called Plastisphere when formed on plastic debris (Zettler et al., 2013, Su et al., 2022).

The monitoring of MPs distribution in coastal ecosystems is crucial for obtaining insights into the transport and accumulation patterns of these particles, which are of utmost importance for the proper management of these pollutants (Kershaw et al., 2015). However, monitoring studies are conducted through sampling efforts, which involve high financial costs and time demands, especially in larger areas. Due to the challenges associated with monitoring this type of solid waste, the numerical modeling approach has emerged as a promising and alternative tool for understanding the distribution of MPs in extensive areas and in the water column (Isobe et al., 2009; Lebreton et al., 2012; Critchell & Lambrechts, 2016; Jálon-Rojas et al., 2019; Díez-Minguito et al., 2020; Baudena et al., 2022). This approach exposes these particles to different physical processes, allowing for tracking and providing insights into their origins, distribution and destinations. Moreover, it contributes to more accurate mapping of potential risk areas and suggests monitoring sites. Numerical models also facilitate the evaluation of hypothetical scenarios and the consistent interpretation of sparse data.

Patos Lagoon is considered the largest choked coastal lagoon in the world (Kjerfve, 1986), serving as a central hub for population, commerce, industry and recreation. As a result, it is also subject to the disposal of industrial and municipal waste. According to Santos et al., (2023), between the years 2010 and 2017, the annual input of plastic waste into Patos Lagoon was estimated between 21.67 and 107.19 thousand tonnes, with the main polymers found being Polypropylene (PP), Polyethylene (PE), and Polyvinyl Chloride (PVC). In the estuarine area is located the second largest harbor of Brazil, Rio Grande Harbor. This industrial area is responsible for the transport and operation of up to 50 million tons per year, subjecting this region to large amounts of urban waste (Pinheiro et al., 2021).

Recent studies have highlighted the occurrence of plastic debris in different areas of Patos Lagoon (Fig. 1) (Silva & Sousa, 2021; Alves et al., 2022; Pinheiro et al., 2022; Santos et al., 2023). Rodriguez et al. (2024) simulated the export of MPs through the Patos Lagoon coastal plume and their accumulation tendency in the coastal zone, but despite these efforts, studies focusing on the transport of MPs in the lagoon main water body remain limited due to its length (240 km). In this context, the aim of this study was to investigate the advection and dispersion transport process of both low and high-density MPs in Patos Lagoon, considering contrasting meteoceanographic conditions and high-density MPs resulting from biofouling formation and its implications for the transport patterns. This study was carried out with the TrackMPD model.

## 2. MATERIAL AND METHODS

### 2.1 STUDY AREA

Patos Lagoon is a shallow coastal plain choked lagoon located in southern Brazil (30° – 32° S, 50°– 52° W) (Fig. 1). With an area of approximately 10.230 km², extending over 240 km, and with an average depth of 5 m, the lagoon drains a basin of 200.00 km². Predominantly consisting of freshwater, the main body of the lagoon experiences coastal water influence within the initial 60 km from the lagoon's mouth, defining the Patos Lagoon Estuary (Fig. 1C). The estuarine area is the deepest region of the system due to the presence of natural and artificial channels (Möller et al., 2001), and it is also the only connection to the Atlantic Ocean through a long (20 km) and narrow (500 m) channel fixed by a pair of 4 km long jetties (Fig. 1C) (Franzen et al., 2023).

The lagoon hydrodynamics is driven by continental discharges and the action of both remote and local winds (Moller et al., 2001; Vaz et al., 2006). The main tributaries of the lagoon are Guaíba and Camaquã rivers and São Gonçalo Channel. The continental discharges in the lagoon have seasonal variability typical of mid-latitudes, with high discharges in austral winter and late spring and low discharges during austral summer and fall and with interannual (Távora et al., 2020) and interdecadal variations (Bortolin et al., 2022). The lagoon is also under the influence of ENSO cycles, resulting in higher (El Niño) or lower (La Niña) precipitation and continental discharges (Távora et al., 2019).

Although the lagoon circulation is influenced by both local and remote wind effects, the local winds act as the primary driving force of the main lagoon body (Fig. 1B) when discharges are < 2000 $m^3.s^{-1}$, producing a set-up/set-down mechanism. Meanwhile, non-local winds tend to promote the exchanges between the estuarine area and the adjacent continental shelf (Fig.1C) due to the Ekman Transport acting 90$^o$ of the wind direction. Throughout the year, northeasterly (NE) winds dominate, while southwesterly (SW) become more important during autumn and winter, as frontal systems become more frequent (Möller et al., 2001). This regional wind pattern coincides with the main axis of the lagoon (NE – SW). Moller et al. (1996) indicated that easterly (E) winds occurring during summer and spring are a result of sea breezes.

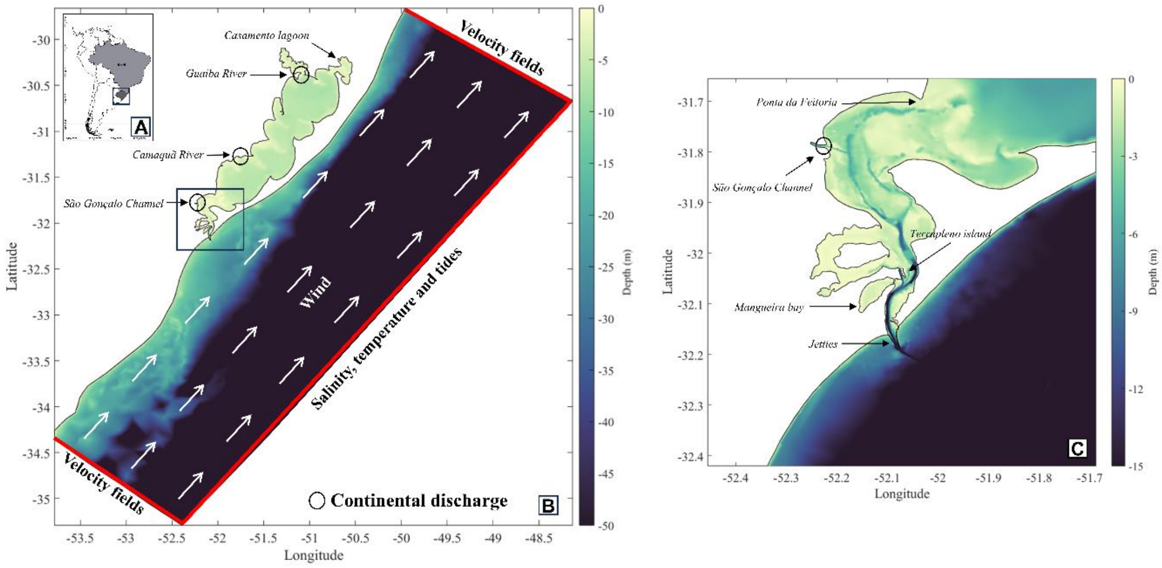


Figure 1: Study area (A, B, C). Model domain with the main tributaries of the lagoon (outline dots), bathymetric information represented in the color scale, identification of open boundaries, and applied boundary conditions for the simulations (B). Patos Lagoon estuary (C).

## 2.2 HYDRODYNAMIC MODEL

The TELEMAC-3D hydrodynamic model, version V7P0, was applied (http://www.opentelemac.org) to generate the advective field for the MPs dispersion simulations with TrackMPD. TELEMAC-3D was developed by the Laboratoire National d'Hydraulique (LNH) of Electricite de France (EDF). Based on the Finite Element Method, it solves the Reynolds averaged three-dimensional Navier-Stokes equations, considering local variations in the free surface of the fluid over time and hydrostatic pressure, in addition to Boussinesq approximations to solve the motion equations (Hervouet, 2007). The resulting equations are suitable for application in shallow waters, where vertical fluid velocities are much smaller than horizontal velocities. Advection and diffusion equations are used for calculating the transport of tracers such as temperature, salinity and suspended sediment. The key outcomes obtained at each point of the numerical grid include velocities in the three directions (*u*, *v*, and *w*), concentrations of transported tracers, and the elevation of the free surface of the fluid.

The numerical domain of the model encompasses the entire lagoon and extends to a depth of 2.300 m in the adjacent coastal region (Fig. 1B), being discretized through a non-structured grid of finite elements that allows more control of the element distribution within the domain, and consequently, more autonomy to establish finer resolution in regions with complex morphology or bathymetry. Vertical discretization was achieved through 7 sigma layers. The non-structured grid used in this study comprises 52.098 points and was generated through the BlueKenue software, version 3.3.4, (https://nrc.canada.ca/en). The hydrodynamic performance of TELEMAC for the study area has been extensively calibrated and validated by various authors (Fernandes et al., 2002, 2005, 2007, 2021; Bitencourt et al., 2020, Lisboa et al., 2022, Franzen et al., 2023), consistently showing good to excellent results for both RMSE and RMAE. The resulting grid has already been calibrated and validated by Silva et al. (2002), who also presents details about the configurations used for this simulations.

Initial and boundary conditions for the numerical grid were extracted from different sources, interpolated, and prescribed at the respective open boundaries of the grid (Fig. 1B). Throughout the three-dimensional domain, initial fields of salinity and temperature were prescribed based on the results of the Hybrid Coordinate Ocean Model (HYCOM, https://hycom.org) + NCODA, which have a temporal resolution of 1 day and a spatial resolution of 1/12°. Initial concentrations of suspended sediment were considered null throughout the domain. The OSU Tidal Inversion System (OTIS) was used for prescribing sea surface elevation at oceanic boundaries. Sea surface elevation is calculated by the inverse solution of Laplace's equations for tidal dynamics, using data collected by the TOPEX/POSEIDON Project, internally available in the TELEMAC-3D model. To obtain a reliable estimate of sea surface elevation, 33 tidal harmonic components were considered. Once the sea surface elevation is known at one edge point, the Continuity Equation is integrated, and the components of current velocity are obtained. At the surface boundary, the numerical grid was forced with results from the global ECMWF model (European Center for Medium-Range Weather Forecast, http://www.ecmwf.int), with a temporal resolution of 24 h and spatial resolution of 0.75°. At the continental boundaries, daily river discharge data from the National Water Agency (ANA, http://www.ana.gov.br) for Guaíba River and Camaquã River were used. For the São Gonçalo Channel discharge, water level data obtained from the Mirim Lagoon Agency (ALM, https://wp.ufpel.edu.br/alm/agencia) were used and transformed into daily discharge from a rating curve (Oliveira et al., 2015).

The period of interest for our study corresponds to the entire year of 2013 (365 days), saved every 24 hours. This specific year was chosen based on the Oceanic Niño Index (ONI) analysis, where it appears as a neutral year with respect to the warm and cold phases of the ENSO phenomenon. Therefore, selecting the year 2013 allows studying the MPs transport process in the Patos Lagoon and its estuary under hydrodynamic conditions without the influence of the ENSO phenomenon. To accomplish this, the hydrodynamic model results were used to force the TrackMPD model (Jalón-Rojas et al., 2019).

## 2.3 LAGRAGIAN TRACKING MODEL

The Tracking Marine Plastic Debris model (TrackMPD, Jálon-Rojas et al., 2019), is a particle transport model that accepts current velocities from various hydrodynamic models such as MOHID, POM, MARS, NEMO, and TELEMAC-3D. The hydrodynamic velocities that the model supports can result from the discretization of structured or unstructured grids. Regarding the vertical discretization of the domain, TrackMPD accepts hybrid vertical coordinates (z-σ) and sigma coordinates (σ), depending on the settings used in the hydrodynamic model. It takes into account the physical characteristics of each type of plastic, such as size, shape, particle density and settling velocity. Additionally, processes influencing the behavior and transport of MPs, such as advection, turbulence, deposition, beaching, resuspension, biofouling, and degradation, can be independently added to the model, according to the purpose of the study.

TrackMPD can be used in both 2D and 3D modes. Its operation occurs in two stages, where the first involves the integration and storage of velocity fields derived from the hydrodynamic model, and the second consists of simulations involving the calculation of particle trajectories. Once the velocities have been converted to TrackMPD's standard input formats (step 1), different simulations can be conducted using various model configurations (step 2), without the need for new integrations of the hydrodynamic results.

As the model is based on a Lagrangian approach, each particle is advected using the velocity fields, where the latter is interpolated in both time and space for the particle's location. Advection can be calculated using the second or fourth-order Runge-Kutta method (RK2 and RK4). Higher orders in the method, despite exhibiting better precision, entail higher computational costs. Additionally, considering the temporal and spatial scales of the studied physical problem, it is necessary to configure the integration time interval for the calculation of particle advection. TrackMPD resolves calculations at two integration timescales, an external and an internal one. The external timestep ($\Delta t_e$) is derived from the hydrodynamic model and corresponds to its outputs (e.g., results every 24 h). The internal timestep ($\Delta t_i$) is used for calculating particle trajectories (e.g., 30 minutes). To compute advection accurately and avoid an exaggerated estimate of particle displacement, it is recommended to use a smaller internal timestep compared to the external one.

The behavior of particles in the water column depends on their physical characteristics, which determine their settling velocity ($w_s$, m.s$^{-1}$). Settling velocity occurs when the gravitational force, minus the particle's buoyancy, is greater (smaller) than the drag force. Thus, particles exhibit positive buoyancy (rise) or negative buoyancy (settling). The settling velocity of MPs can be constant or vary over time due to the influence of degradation and biofouling formation, among other processes. Therefore, particle trajectories in a three-dimensional domain are determined by advection, diffusion, and their vertical displacements through the following equations:

$$dX(t) = dX_{adv}(t) + dX_{diff}\,(t) = U(x, y, z,t)dt + dX'(t) \quad (1)$$

$$dY(t) = dY_{adv}(t) + dY_{diff}\,(t) = V(x, y, z,t)dt + dY'(t) \quad (2)$$

$$dZ(t) = dZ_{adv}(t) + dZ_{diff}\,(t) + dZ_{dep}(t) = W(x, y, z,t)dt + dZ\,'(t) - ws\,(t)dt \quad (3)$$

where $dX_{adv}$ = ($dX_{adv}$, $dY_{adv}$, $dZ_{adv}$) represents advection established in the zonal (x), meridional (y), and vertical (z) axes obtained through the velocity fields of the hydrodynamic model U = (U, V, W). Turbulent diffusion $dX_{diff}$ = ($dX_{diff}$, $dY_{diff}$, $dZ_{diff}$) is represented by a random component dX’ = (dX’, dY’, dZ’) added to the particle's movement on a much smaller scale than the advection movement. Vertical displacements $dZ_{dep}$ depend on the settling velocity ($w_s$) of MPs.

It is also possible to calculate the settling velocity through formulations provided in the model, which result from experiments involving MPs (Khatmullina & Isachenko, 2017; Waldschlager & Schuttrumpf, 2019; Jalón-Rojas et al, 2022). These experiments serve as a basis for more realistic parameterizations of the variables. Through these formulations, it is also possible to include the effect of biofouling on particles, which alters the settling velocity ($w_s$). By defining a biofilm growth rate as a function of time, it is possible to calculate the density rate varying over time (g.cm$^3$.day), defined as:

$$Ps = P_0 + DR\Delta t_i$$

where $P_0$ is the polymer density, $\Delta t_i$ is the internal timestep, responsible for calculating displacements, and *DR* is the biofilm growth rate as a function of time. A more detailed description of the model's equations and all available numerical processes and solutions is presented by Jálon-Rojas et al. (2019). The TrackMPD validation for Patos Lagoon is presented by Rodriguez et al. (2024). Simulations were carried out using TrackMPD version 2.2.

## 2.4 DENSITY PROBABILITY MAPS

Using a statistical approach to better highlight the accumulation trends of MPs (hotspots), results from the TrackMPD model were analyzed through probability density maps, calculated using probability density functions (PDFs). These density maps provide a visual representation of potential regions of MP accumulation in the system, identifying areas with the highest probability of particle occurrence. According to Mitarai et al. (2009), this type of analysis can be applied to determine expected tracer concentrations, widely used for predicting dispersion patterns. The functions are calculated based on the probability of a particle moving from one location to another during a time interval, counting the number of particles per interval and subsequently normalizing by the total number of the particles, mapping these through the grouping of particle positions into histograms (Jálon-Rojas et al., 2019). The PDFs were calculated at a grid resolution of approximately 0.03 km$^2$.

## 2.5 SIMULATIONS SETUP

The simulations were carried out considering high (scenarios 2 and 4) and low (scenarios 1 and 3) continental discharge in Patos Lagoon (Tab. 1). In Scenarios 1 (low discharge) and 2 (high discharge) the trajectories of low-density MPs were simulated considering the entire lagoon, with MPs particles being released from the three main tributaries of the system (Guaíba and Camaquã rivers and São Gonçalo Channel).

According to Santos et al. (2022), an estimate of the contribution of plastic waste from the tributaries into Patos Lagoon suggests that Guaíba and Camaquã rivers, and São Gonçalo Channel introduce percentage contributions of 60%, 20%, and 20% of the total load of plastic waste into the system, respectively. Thus, for Scenario 1 and 2, covering the entire lagoon, 2.000 particles were proportionally distributed among the three tributaries (1.200, 400 and 400), and for Scenario 3 and 4, 400 particles were released from São Gonçalo Channel (Tab 1). The authors also reported that among all types of plastics described, the most abundant type was polypropylene (PP), which corroborates with the results described by Rodriguez et al. (submitted). Therefore, in all simulated scenarios, the chosen polymer type was PP.

For scenarios 1 and 2 in the main lagoon, the only physical processes taken into account were advection and dispersion. For Scenarios 3 and 4, the transport and accumulation of high-density MPs were simulated considering only the estuarine area, with MPs being released only from São Gonçalo Channel. In these scenarios (3 and 4), in addition to advection and dispersion, the biofouling process was also included in the configuration setup, aiming to indicate the trajectory of high-density MPs. High-density MPs, represent those subject to biofouling, included here to better understand how this phenomenon influences MP dynamics in Patos Lagoon estuary. This decision was driven by the recognition that estuarine regions often exhibit more pronounced interactions with marine currents, which can significantly influence the fate and transport of high-density MPs. In all scenarios, the horizontal coefficient ($K_h$) used were set up to 1, a typical value for coastal systems (Jálon-Rojas et al., 2019). For scenarios involving high-density MPs, biofouling rate (*DR*) was set to 0.0005 $g.cm^{-1}.day^{-1}$ (Jálon-Rojas et al. 2019). Simulations were run at a 5-minute internal timestep ($\Delta t_i$), and only the horizontal displacements due to advection and dispersion were taken into account when presenting the results.

Table 1: Simulations setup for the scenarios considering low-density MPs in the entire lagoon (1 and 2) and high-density MPs in the estuary only (3 and 4).

| | Scenarios | | | |
|---|---|---|---|---|
| | ***1*** | ***2*** | ***3*** | ***4*** |
| Domain | Lagoon | Lagoon | Estuary | Estuary |
| Discharge | Low | High | Low | High |
| Tributaries | Gua/Cam/SãoG | Gua/Cam/SãoG | SãoG | SãoG |
| MP type / density | PP/ low | PP/ low | PP/ high | PP/ high |
| Number of MPs released from each tributary | 1.200/ 400 / 400 | 1.200/ 400 / 400 | 400 | 400 |
| Predominant wind | NE | SW | NE | SW |
| Biofouling rate | No | No | 0.0005 | 0.0005 |

# 3 RESULTS

## 3.1 HYDRODYNAMICS DURING LOW AND HIGH DISCHARGE PERIODS

The analysis of the hydrodynamic conditions during the simulations serves as the starting point for understanding the MPs dynamics in the system. The hydrodynamics of the lagoon was assessed using information about the winds (Fig. 2A and 2B), freshwater discharge from the tributaries (Fig. 2C and 2D) and resulting current velocity under predominant wind conditions (Fig. 3).

During the low discharge period (Fig. 2C), maximum values (2.000 $m^3.s^{-1}$) occurred in Guaíba river, and smaller contributions from Camaquã river (600 $m^3.s^{-1}$) and São Gonçalo Channel (500 $m^3.s^{-1}$) (Fig. 1). Winds were predominantly from the north quadrant (Fig. 2A). The highest (lower) wind velocities occur from the NE (E) direction, with speeds exceeding 6 $m.s^{-1}$ (2 $m.s^{-1}$).

For simulations during the high discharge period (Fig. 2D), the maximum discharge occurred in Guaíba river (8.000 $m^3.s^{-1}$) and remained high during all the simulation. The same occurs for the Camaquã river, which reached 3.000 $m^3.s^{-1}$, but not to São Gonçalo Channel, which maintained low discharges (800 $m^3.s^{-1}$) throughout the simulation (Fig. 2D). Winds during this period presented greater variability (Fig. 2B), with prevailing wind direction (SW-NE) aligns with the main axis of the lagoon and wind speeds of 9 $m.s^{-1}$ and 7 $m.s^{-1}$ from the SW and NE directions, respectively (Fig. 2B).

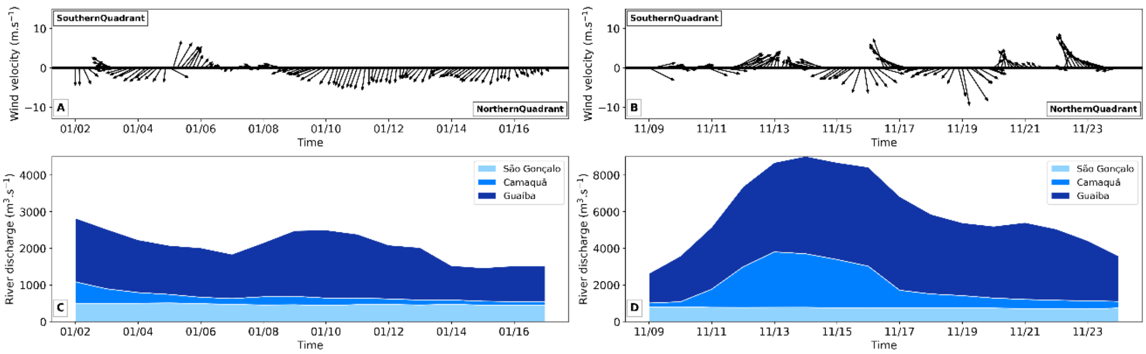


Figure 2: 3-hour wind velocity and direction during low (A) and high discharge (B) simulated periods, where positive (negative) values represent winds from the south (north) quadrant. Discharges of the three main tributaries of Patos Lagoon during low (C) and high (D) discharge.

Figure 3 presents the resulting current velocity fields under the predominant wind directions NE (Fig. 3AB) and SW (Fig. 3CD) observed during the low and high discharge simulations.  In the main lagoon water body, the lowest velocities occurred during both low and high discharge (Fig. AC). In the estuarine region, NE (SW) winds promoted more intense ebb (flood) currents, especially in the access channel, where the highest velocities occurred (Fig. 3BD). The impact of the winds on the currents is evident, along with the notably higher current velocities within the estuarine region compared to the northern sector of the lagoon. It is also possible to observe that through this wind pattern, more intense currents are observed along the margins of the lagoon body.

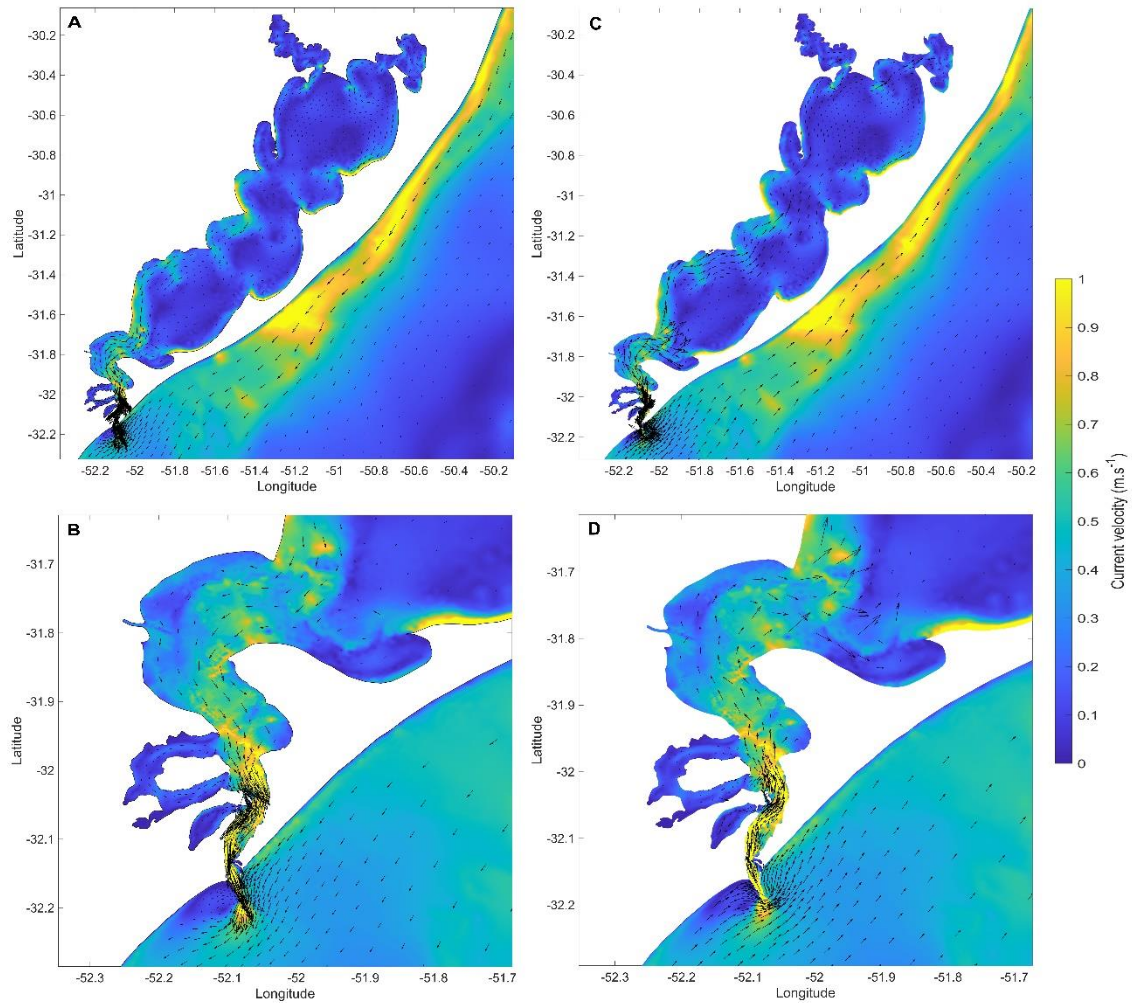


Figure 3: Current intensity and direction in Patos Lagoon during Northeast (AB) and Southwest (CD) wind events. Letters B and D represent the estuarine area.

## 3.2 LOW-DENSITY MICROPLASTICS TRANSPORT IN THE LAGOON (SCENARIOS 1 AND 2)

Figure 4 shows the trajectories of the low-density MPs together with their respective velocities (color scale) during the periods of low (Figs. 4A and 4B) and high (Figs. 4C and 4D) discharge in the entire lagoon. During the simulated period, it was observed that the 1200 MPs released from Guaíba river remained in the north of the system, with small dispersion towards the central lagoon. This is highlighted by the low MPs velocities, where most of them did not reach 0.2 $m.s^{-1}$. Notably, only those MPs reaching the lagoon's shores exhibited higher velocities (0.5 $m.s^{-1}$). Therefore, even with the predominance of northeast winds (Fig. 2A), the combination between the winds and low discharge (Fig.

2C) were not enough to enable a significant transport of MPs from the Guaíba river towards the central region of the lagoon.

During the high discharge period (Figs. 4C and 4D), the dynamics of MPs released by the Guaíba river is more intense. In the early stages of the simulation, a predominance of westerly winds was observed (Fig. 2B), which, combined with the high discharge provided by Guaíba river (Fig. 2D), imposed a transport of MPs towards the eastern margin of the lagoon in the northern region, reaching velocities of 0.7 $m.s^{-1}$. However, similarly to the behavior observed in the low discharge period (Figs. 4A and 4B), the center of the northern cell continues to exhibit MPs with low velocities (0.1 $m.s^{-1}$). At the end of the simulated period, the majority of MPs released from the Guaíba river was directed southward, reaching the central region of the lagoon, while the others remained trapped due to the low cellular circulation in the northernmost portion of the lagoon.

During the low discharge period, the 400 MPs released from Camaquã river were mainly transported along the western margin of the lagoon, where the higher MPs velocities (0.3 $m.s^{-1}$) were observed, reaching the estuarine area (Figs. 4A and 4B). When arriving at the estuary limit, MPs dispersed near the morphological step that separates the main body of the lagoon from the estuary, known as Ponta da Feitoria (Fig. 1C), indicating that this formation acted as a barrier to the transport of MPs towards the estuary. Subsequently, with the prevailing north quadrant winds, currents towards the south prevailed and some MPs entered the estuary via the western margin, reaching the coastal region. Due to the low discharge from the Camaquã river during the simulated period (Fig. 2C), wind prevailed as the main contributor to the transport of MPs during this period.

During high discharge period, however, the majority of MPs released from Camaquã river remained trapped within the recirculation of the lagoon south cell. Furthermore, the western margin near the mouth of Camaquã river was where the MPs exhibited higher velocities, reaching up to 1 $m.s^{-1}$. In the central part of the south cell MPs particles remained with low velocities (0.1 $m.s^{-1}$).

Considering the 400 MPs released from São Gonçalo Channel during the low discharge event, it is clear that they encountered stronger currents (Fig. 3) and dispersed south reaching the coastal area with high velocities (Figs. 4A and 4B). Due to the low discharge from the São Gonçalo Channel (Fig. 2C) during this period, the transport of MPs occurred based on the influence of the predominant NE wind (Fig. 2A). However, as MPs approach the narrow 20 km long access channel, the funneling effect intensifies the currents and it is possible to observe higher velocities of MPs near the mouth (0.8 $m.s^{-1}$) (Fig. 4B). It is important to observe that some MPs enter the shallow bays of the estuary.

When looking at the high discharge period (Fig. 4BC), MPs released from São Gonçalo Channel also reached the coastal area (Fig. 4D). It was also noticeable that almost the entire estuarine area exhibited MPs with high velocities, differing only where they moved to shallower areas and towards the margins. These pronounced displacements of MPs corresponded to the stronger currents that occurred in this area (Fig. 3B). Even with the wind varying in direction during the simulated period (Fig. 2B), the predominant direction of the MPs trajectories was NE, promoting ebb flows towards the coastal area. Some MPs particles were also observed in the estuary shallow bays.

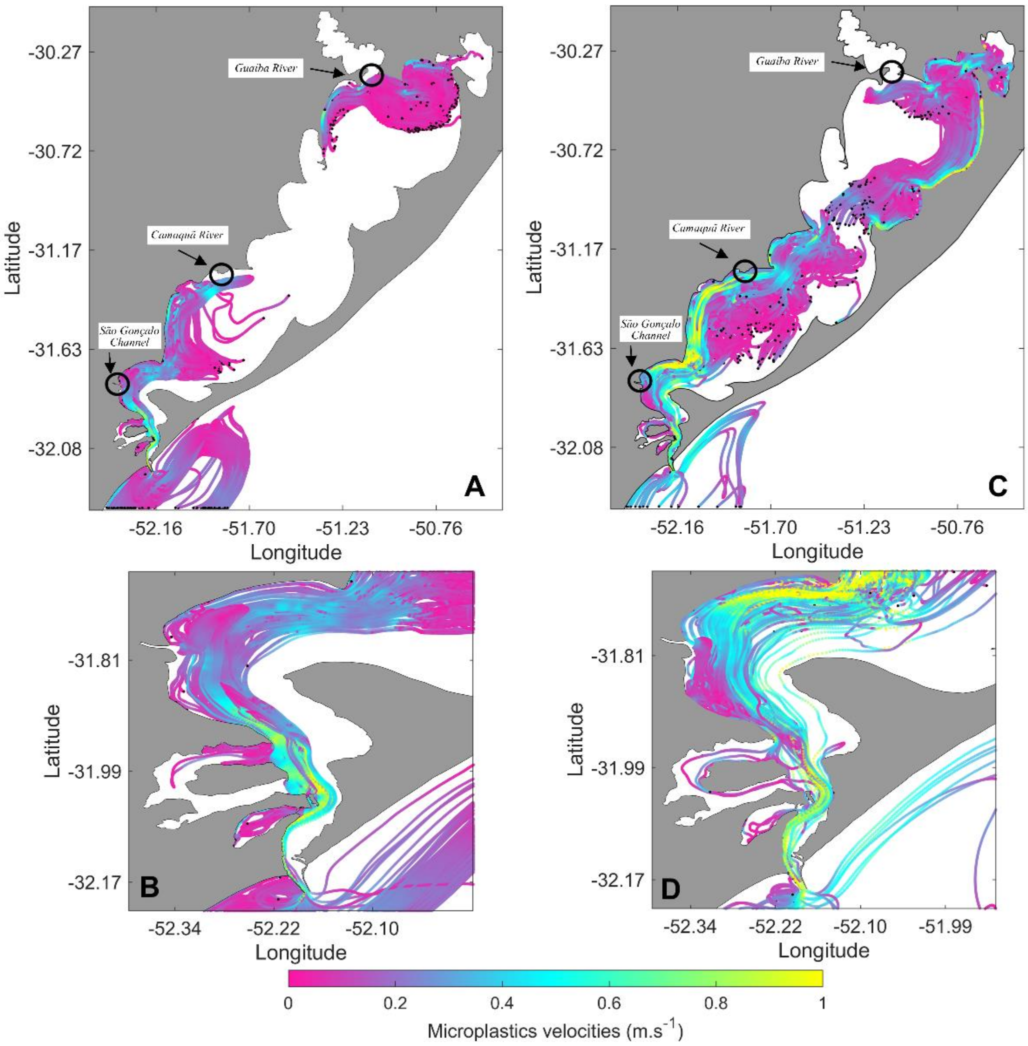

Figure 4: Trajectories of low-density MPs during low (A, B) and high (C, D) discharge. Letters B and D indicate the estuarine area. Color bar indicated microplastics velocities during trajectories and no-fill makers the release sources.

## 3.3 HIGH-DENSITY MICROPLASTICS TRANSPORT IN THE ESTUARY (SCENARIOS 3 AND 4)

Considering the presence of biofouling on the MPs, 400 high-density MPs particles were released from São Gonçalo Channel during the low discharge period (Fig. 2C). Results indicated that throughout the simulated period, MPs remained restricted to the upper estuarine region, near their release location (Fig. 5A). Although they were in an area of higher currents (Fig. 3A) and predominant NE winds (Fig. 2A), their dispersion was small. Consequently, MPs velocities were also small compared to the other scenarios, reaching 0.1 $m.s^{-1}$. In the end of simulated period, no MP reached the coastal area or even the lower estuarine region.

In the high-discharge period (Fig. 5B) the high-density MPs also remained close to their release area, with small dispersion. Even with a greater prevalence of SW winds (Fig. 2B), which configure flood currents in this region (Fig. 3B), they had little influence on the trajectories. However, unlike what happens during the low discharge period (Fig. 5A), during high discharge, the velocities of the MPs generally increase, with some particles reaching 0.2 $m.s^{-1}$, while the others remained constant in 0.1 $m.s^{-1}$. Just like in low discharge, at the end of the simulated period, no MP reached the coastal area.

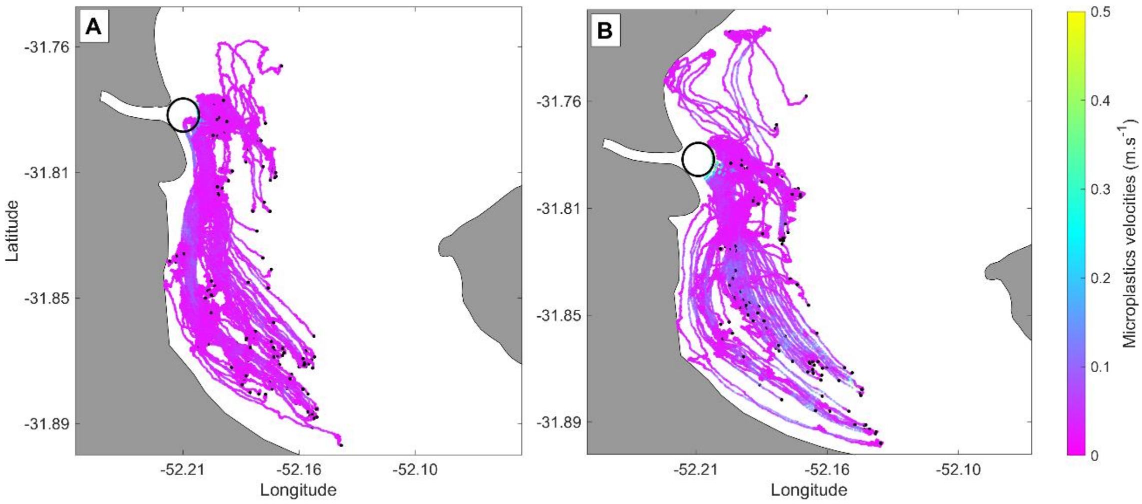


Figure 5: Trajectories of high-density MPs released from São Gonçalo Channel during the low (A) and high (B) discharge simulations. Color bar indicated microplastics velocities during trajectories and no-fill makers the release source.

### 3.4 HOT SPOTS - POTENCIAL ACCUMULATION AREAS

Figure 6 present the probability of MPs accumulation in Patos Lagoon (hot spots), considering both low and high-density MPs simulated during period of low freshwater discharge. Results of the PDF analysis for the low discharge period (Fig. 4A and Fig. 5A), indicated higher likelihood of MPs hot spots occurrence in the three regions of the main lagoon (Fig. 6A): in the northern area of the lagoon, in the central cell close to Camaquã river mouth and in the morphological step at Ponta da Feitoria (Fig. 1C). In the estuarine area, a large number of hot spots was observed, mainly near the São Gonçalo Channel mouth. Furthermore, hot spots were also observed in the lower estuarine region and towards its mouth, especially near Terrapleno Island and around the mouth of Mangueira Bay (Fig. 6B). It was also possible to observe hot spots on both sides of the West Jetty (Fig. 6C).

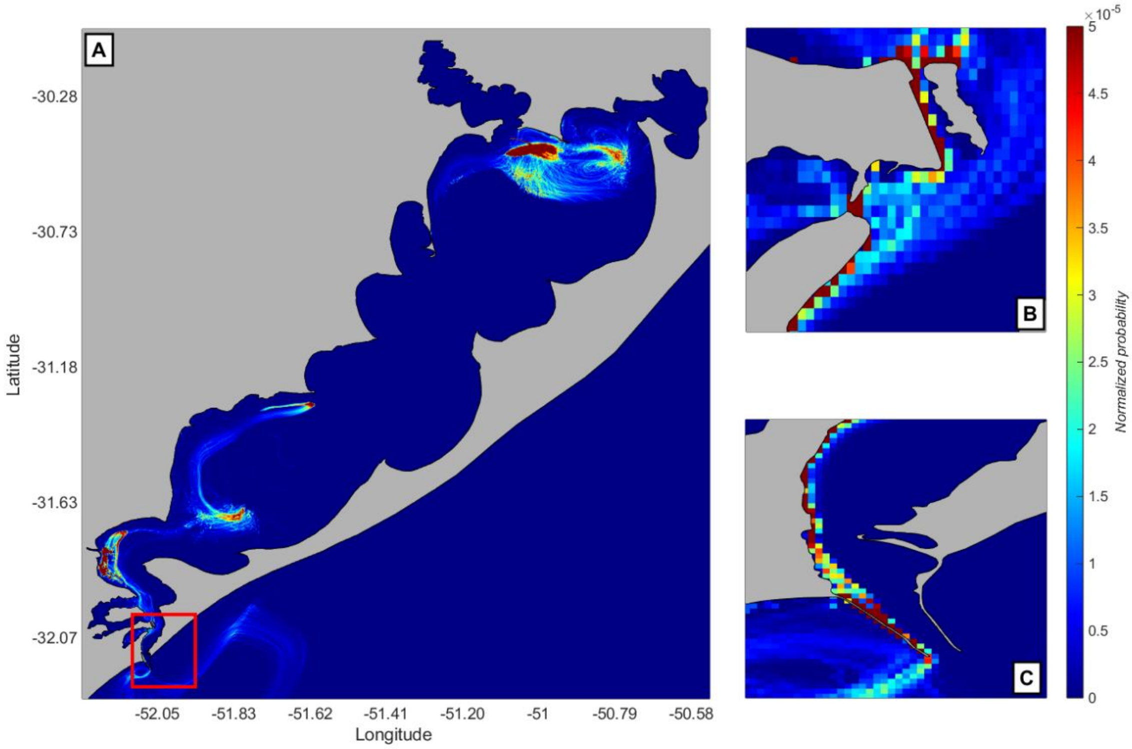


Figure 6: Density maps from low and high density microplastics simulated during a low discharge period. Letters B and C represent the zoom in the red square, where letter B encompasses the region of Terrapleno Island, and letter C covers the area of the West Jetty. The color bar indicates the normalized probability values from the density maps.

The probability of hot spots of MPs during the high discharge period when considering low (Figs. 4C and 4D) and high-density MPs (Fig. 5B) is presented in Figure 7'. Results indicated hot spots of MPs near the mouth of Guaíba river (Fig. 7A) and in the northeastern region of Patos Lagoon (Fig. 7B)**.** Some hot spots were also observed on the west margin of the south cell due to the Camaquã river contribution. The estuarine area also has hot spots near the mouth of São Gonçalo Channel (Fig. 7A), similarly to the low discharge period (Fig. 6A). Other estuarine MPs hotspots were observed at the western jetty.

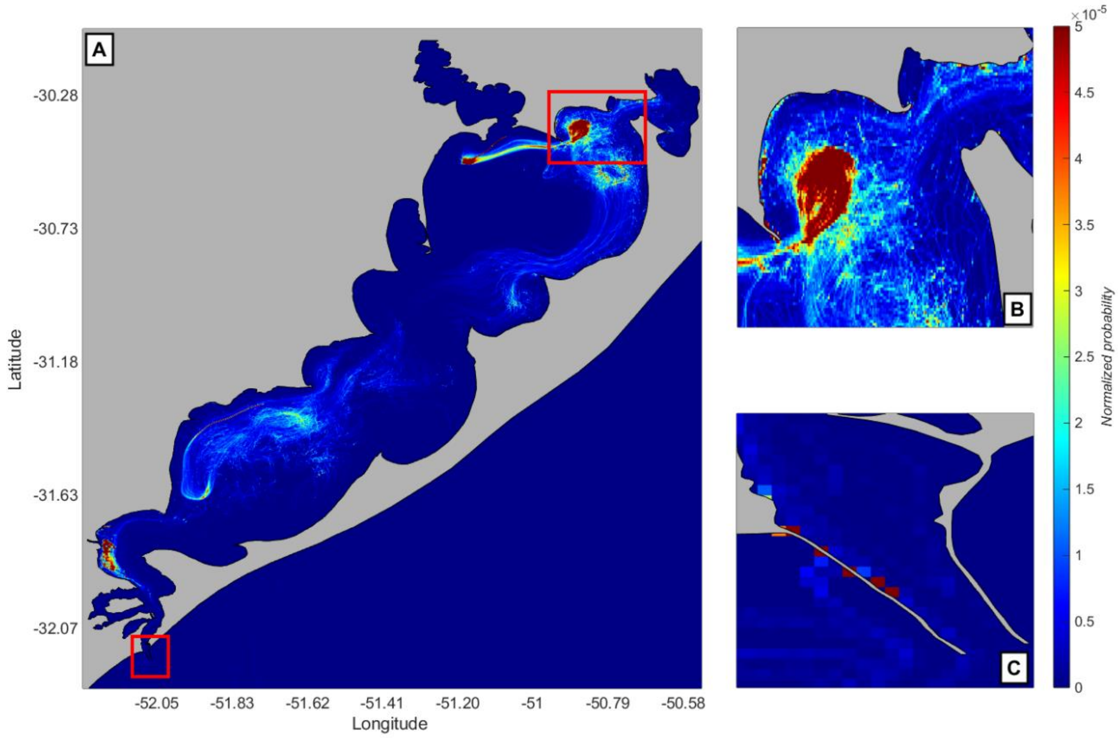


Figure 7: Density maps from low and high density microplastics simulated during the high discharge period. Letters B and C represent the zoom in the red square, where letter B encompasses the region around the mouth of Casamento lagoon, and letter C covers the area of the West Jetty. The color bar indicates the normalized probability values from the density maps.

## 4. DISCUSSION

### 4.1 Low-density microplastics transport in the lagoon (scenarios 1 and 2)

Simulation results considering only low-density microplastics (Fig. 4) demonstrated that the calculated trajectories for MPs were consistent with variations in wind, discharge (Fig. 2) and current (Fig. 3) regimes calculated by the hydrodynamic model. Both in the central and estuarine regions, MPs exhibited greater dynamics, managing to reach the coastal area. Furthermore, the different distribution of MPs among the northern, central, and southern sectors of the lagoon also proved to be coherent with the recognized regions of higher and lower hydrodynamics in the lagoon (Paim & Möller, 1986; Niencheski et al., 1988). These authors observed weaker currents in the northern and southern cells and more intense ones in the central region of the lagoon, corresponding to a node of a standing wave established in the main lagoon body due to local wind action (Moller et al., 2001). Additionally, stronger currents are usually observed on the western margin of the lagoon. This behavior explains the observed transport of MPs and is consistent with the results presented by Bortolin et al. (2020) regarding the formation of mud depocenters in the lagoon.

In the low discharge simulated period (Fig. 4AB), it can be summarized that MPs released in the northern part of the lagoon showed a tendency to become trapped within the system, while those released in the central region tended to remain primarily in the estuarine area, with some exportation to the coastal region. The transport of the debris in the north was aligned with the low hydrodynamics in the northern cell of the system. They exhibited little displacement along the main axis of the lagoon, primarily following the western margin. Thus, during the simulated period of 15 days, none of the MPs particles released in the northern lagoon reached its central region.

MPs released in the estuarine region exhibited a tendency for exportation to the adjacent coastal area. This transport was favored by the interaction between the estuary's geometry and the ebb and flood flows driven by barotropic pressure gradients established due to river discharge and wind (Moller et al., 2001). This barotropic circulation pattern was also observed by Schicchi et al. (2023), where it was also indicated that the trajectories of MPs located near river mouths responded markedly to continental discharge. However, in our case, considering MPs distribution from Guaíba river this did not happen. In this region, surface circulation was considered low regardless of the wind or discharge. MPs exported to the coastal area through the access channel had a tendency to either remain defined or indefinitely in the recirculation region that occurs south of the western jetty. Cohen et al. (2019) indicated that the concentration of low-density MPs varied spatially due to surface circulation. Considering these factors, the distribution of MPs relies significantly on the flow field.

During the high discharge period (Fig. 4CD), the behavior of MPs differed from that observed during low discharge (Fig. 4AB). It was possible to observe greater displacements of MPs released from the Guaíba river towards the main axis of the lagoon. These pronounced displacements were a response to the higher discharge combined with the wind action. MPs with high velocities moved along the edges of the lagoon, both on the eastern and western shores. Those located in the central regions of the lagoon exhibited lower velocities associated with their shorter displacements. This may be attributed to the extent of the lagoon and its cellular morphology, facilitating the entrapment of particles within the circular dynamics of the region. Also, this distinct behavior can be explained by the hydrodynamics of the lagoon itself. The higher velocities along the margins create a pathway for the MPs in response to the wind action. However, as they move towards the central areas of the lagoon, the transport of debris slows down with velocity.

However, in the estuarine region, favored by the narrowing of the access channel towards the estuary mouth, the behavior of MPs responds to the variability of the system. Microplastics are exported more intensely and rapidly towards the coastal region during these periods of low hydrodynamic activity. Summers et al. (2023) indicated that there is an increase in MPs accumulation within the bay during low hydrodynamic periods, whereas the opposite effect expels debris from the area, which corroborates with the results indicated in our region.

### 4.2 High-density microplastics transport in the estuary (scenarios 3 and 4)

Considering biofouling-affected microplastics (high density), in both low and high discharges, MPs released from São Gonçalo Channel exhibited a markedly different behavior from those free from biofouling action. The difference was evident for low-density MPs in the estuarine region (Fig. 4BD) compared to results from biofouling-affected MPs (Fig. 5 AB). Regardless of the wind direction and discharge, MPs remained confined within the upper estuary, exhibiting minimal displacement and velocities. When comparing biofouling-free MPs to those affected by this process, it becomes evident that this process strongly influences the dynamics of MPs. Summers et al. (2023) suggested that MPs with lower density had more tendency to be exported to the continental shelf, while higher-density MPs took significantly longer to be exported, remaining trapped within estuaries for extended periods. The authors findings also corroborate with our results when we take into count the trajectories of MPs from all 4 scenarios. Furthermore, by concentrating our efforts on the estuarine zone, we aimed to capture the critical interface between the lagoon and the adjacent oceanic environment, where rapid exchanges and mixing occur. Additionally, it was expected that being considered denser particles, they would have less spatial displacement, thus having a greater tendency to remain within the lagoon body.

### 4.3 Limitations for the study and future work

Despite the lack of specific parameterizations for the study region, the presented results serve as initial indicators of how MPs transportation occurs in Patos Lagoon. Low-density MPs under the influence of a less dynamic system (low discharge, scenario 1) exhibit a trapping gradient from the Guaíba river towards the São Gonçalo Channel. However, when the dynamics of the lagoon become more pronounced in terms of both discharge and wind, MPs show greater displacements from the northernmost region to the mouth of the lagoon throughout the estuary. The variation in MPs concentration, starting from Guaíba river and extending to the open ocean through the estuary, highlights the significant function of Patos Lagoon as a buffer system before MPs are transported from land to sea (Meijer et al., 2021). In regard to dense MPs, the plastisphere played a significantly more prominent role than the influence of wind and discharge. It is plausible to infer that Rdisplayed a tendency to remain trapped near their release region. Consequently, considering the presence of the plastisphere suggests that the estuary could potentially act as a short-term sink rather than a source of microplastics for the adjacent coastal region, as shown in Figure 5. Despite this retention gradient, upon analyzing the density maps, it was possible to observe that the estuarine region is the area with the highest probability of occurrence of these particles.

It is crucial to emphasize that the results presented in this study stem from the chosen configurations for the simulations, representing a significant step towards the understanding of the dynamics of MPs and the contribution of the plastisphere effect in this process. The investigation of the plastisphere is innovative and provides a strong foundation for future research in this area. Model simulations still face some limitations regarding the parametrization for dispersions coefficients, computational costs, and model validation. However, future research should focus on these limitations and other simulations should be conducted using increasingly realistic parameterizations (horizontal and vertical dispersion coefficients), incorporating other processes (deposition, bottom drag, resuspension, and degradation (Jalón-Rojas et al., 2019), and different characteristics for MPs particles (Santos et al., 2023; Alves et al., 2023). Furthermore, it is worth noting that the transport of microplastics may exhibit different behavior when considering the positive and negative phases of the ENSO cycle. Higher discharges are expected during El Niño events, suggesting a higher tendency for microplastics to be exported to the coastal region during this period. Conversely, during La Niña years, the opposite process might occur.

## 5. CONCLUSIONS

Low-density MPs exhibited behavior consistent with the hydrodynamics of their respective release regions and dynamic configuration of the lagoon. During low discharge, short-term simulations revealed a gradient of MP retention within the system, with a larger quantity of MPs being retained in the north under the influence of lower discharges and moderate winds. During this period, the estuarine region exhibits the highest dynamics, influencing the increased export of debris to the coastal area. In high discharge periods, MPs exhibited a different dynamic, responding to the configuration of the lagoon. Increased wind activity and continental discharges influenced the larger displacement of the MPs. Unlike in low-discharge, they exhibit higher velocities along the shores of the lagoon body. MPs subjected to biofouling action and released in the estuary exhibited distinct behavior from biofouling-free MPs, remaining retained in the upper estuary in both low and discharge simulations.

Consequently, it is possible to infer that the regions further from the estuary's mouth may be responsible for retaining MPs within the lagoon body. Conversely, the estuarine region tends to facilitate the exportation of low-density MPs to the coastal region through prevailing ebb currents and trap high-density MPs near release locations. However, this area is also impacted by the presence of these debris because everything that enters the lagoon through rivers or poor waste management eventually reaches the estuarine region and remains there for a certain period.

The present study represents a significant advance in assessing the transport patterns of microplastics (MPs) in Patos Lagoon. While acknowledging that the particle model employed has to be further validated, it is crucial to highlight that achieving such a task was not possible due to the high-water level observed in the system during the recent flood events (September 2023 and May 2024). Nevertheless, the findings presented are pivotal in understanding how MPs are transported from different release locations within the system, aligning with the hydrodynamic behavior. These insights contribute to a comprehension of the source-to-sink process, enabling a robust understanding of spatial and temporal patterns in the exportation or retention of MPs within the system.

## 6. REFERENCES

Abel, S. M., Primpke, S., Int-Veen, I., Brandt, A., & Gerdts, G., 2021. Systematic identification of microplastics in abyssal and hadal sediments of the Kuril Kamchatka trench. Environ. Pollut., 269, 116095, doi: https://doi.org/10.1016/j.envpol.2020.116095

Alves, F. L., Pinheiro, L. M., Bueno, C., Agostini, V. O., Perez, L., Fernandes, E. H. L., ... & García-Rodríguez, F., 2023. The use of microplastics as a reliable chronological marker of the Anthropocene onset in Southeastern South America. Sci. Total Environ., 857, 159633, doi: https://doi.org/10.1016/j.scitotenv.2022.159633

Andrady, A. L., 2011. Microplastics in the marine environment. Mar. Pollut. Bull., 62(8), 1596-1605, doi: https://doi.org/10.1016/j.marpolbul.2011.05.030

Auta, H. S., Emenike, C. U., & Fauziah, S. H., 2017. Distribution and importance of microplastics in the marine environment: A review of the sources, fate, effects, and potential solutions. Environ. Int., 102, 165-176, doi: https://doi.org/10.1016/j.envint.2017.02.013

Banik, P., Anisuzzaman, M., Bhattacharjee, S., Marshall, D. J., Yu, J., Nur, A. A. U., ... & Hossain, M. B., 2024. Quantification, characterization and risk assessment of microplastics from five major estuaries along the northern Bay of Bengal coast. Environ. Pollut., 342, 123036, doi: https://doi.org/10.1016/j.envpol.2023.123036

Barnes, D. K., Galgani, F., Thompson, R. C., & Barlaz, M., 2009. Accumulation and fragmentation of plastic debris in global environments. Philos. Trans. R. Soc. B, 364(1526), 1985-1998, doi: https://doi.org/10.1098/rstb.2008.0205

Baudena, A., Ser-Giacomi, E., Jalón-Rojas, I., Galgani, F., & Pedrotti, M. L., 2022. The streaming of plastic in the Mediterranean Sea. Nat. Commun., 13, 2981, doi: https://doi.org/10.1038/s41467-022-30572-5

Bitencourt, L. P., Fernandes, E. H., da Silva, P. D., & Möller Jr, O., 2020. Spatio-temporal variability of suspended sediment concentrations in a shallow and turbid lagoon. Journal of Marine Systems, 212, 103454, doi: https://doi.org/10.1016/j.jmarsys.2020.103454

Bortolin, E. C., Weschenfelder, J., Fernandes, E. H., Bitencourt, L. P., Möller, O. O., García-Rodríguez, F., & Toldo, E., 2020. Reviewing sedimentological and hydrodynamic data of large shallow coastal lagoons for defining mud depocenters as environmental monitoring sites. Sediment. Geol., 410, 105782, doi: https://doi.org/10.1016/j.sedgeo.2020.105782

Bortolin, E. C., Távora, J., & Fernandes, E. H., 2022. Long-term variability on suspended particulate matter loads from the tributaries of the world's largest choked lagoon. Front. Mar. Sci., 9, Article 1-17, doi: https://doi.org/10.3389/fmars.2022.836739

Chubarenko, I., Bagaev, A., Zobkov, M., & Esiukova, E., 2016. On some physical and dynamical properties of microplastic particles in the marine environment. Mar. Pollut. Bull., 108, 105-112, doi: https://doi.org/10.1016/j.marpolbul.2016.04.048

Cohen, J. H., Internicola, A. M., Mason, R. A., & Kukulka, T., 2019. Observations and simulations of microplastic debris in a tide, wind, and freshwater-driven estuarine environment: the Delaware Bay. Environ. Sci. Technol., 53(24), 14204-14211, doi: https://doi.org/10.1021/acs.est.9b04814

Cole, M., Lindeque, P., Halsband, C., & Galloway, T., 2011. Microplastics as contaminants in the marine environment: A review. Mar. Pollut. Bull., 62(12), 2588-2597, doi: https://doi.org/10.1016/j.marpolbul.2011.09.025

Critchell, K., & Lambrechts, J., 2016. Modelling accumulation of marine plastics in the coastal zone; What are the dominant physical processes? Estuar. Coast. Shelf Sci., 171, 111-122, doi: https://doi.org/10.1016/j.ecss.2016.01.036

Díez-Minguito, M., Bermúdez, M., Gago, J., Carretero, O., & Viñas, L., 2020. Observations and idealized modeling of microplastic transport in estuaries: The exemplary case of an upwelling system (Ría de Vigo, NW Spain). Mar. Chem., 222, 103780. https://doi.org/10.1016/j.marchem.2020.103780

Elisei Schicchi, A., Moreira, D., Eisenberg, P., & Simionato, C. G., 2023. Qualitative Study of the Transport of Microplastics in the Río de la Plata Estuary, Argentina, through Numerical Simulation. J. Mar. Sci. Eng., 11(12), doi: https://doi.org/10.3390/jmse11122317

Eriksen, M., Lebreton, L. C., Carson, H. S., Thiel, M., Moore, C. J., Borerro, J. C., ... & Reisser, J., 2014. Plastic pollution in the world's oceans: more than 5 trillion plastic pieces weighing over 250,000 tons afloat at sea. PLoS One, 9(12), doi: https://doi.org/10.1371/journal.pone.0111913

Erkan, H. S., Takatas, B., Ozturk, A., Gündogdu, S., Aydın, F., Koker, L., ... & Engin, G. O., 2023. Spatio-temporal distribution of microplastic pollution in surface sediments along the coastal areas of Istanbul, Turkey. Mar. Pollut. Bull., 195, 115461, doi: https://doi.org/10.1016/j.marpolbul.2023.115461

Fernandes, E. H. L., Dyer, K. R., Moller, O. O., & Niencheski, L. F. H., 2002. The Patos lagoon hydrodynamics during an El Nino event (1998). Cont. Shelf Res., 22(11-13), 1699-1713, doi: https://doi.org/10.1016/S0278-4343(02)00033-X

Fernandes, E. H. L., Dyer, K. R., & Moller, O. O., 2005. Spatial gradients in the flow of southern Patos Lagoon. Journal of Coastal Research, 21(4), 759-769, doi: https://doi.org/10.2112/006-NIS.1

Fernandes, E. H. L., Monteiro, I. O., & Möller Jr, O. O., 2010. On the Dynamics of Mangueira Bay—Patos Lagoon (Brazil). Journal of Coastal Research, (10047), 97-107, doi: https://doi.org/10.2112/1551-5036-47.sp1.97

Fernandes, E. H., da Silva, P. D., Gonçalves, G. A., & Möller Jr, O. O., 2021. Dispersion plumes in open ocean disposal sites of dredged sediment. Water, 13(6), 808, doi: https://doi.org/10.3390/w13060808

Forero-López, A. D., Rimondino, G. N., Truchet, D. M., Colombo, C. V., Buzzi, N. S., Malanca, F. E., ... & Fernández-Severini, M. D., 2021. Occurrence, distribution, and characterization of suspended microplastics in a highly impacted estuarine wetland in Argentina. Sci. Total Environ., 785, 147141, doi: https://doi.org/10.1016/j.scitotenv.2021.147141

Franzen, M. O., Silva, P., Siegle, E., & Fernandes, E. H., 2023. Influence of long jetties on estuarine and coastal hydrodynamics in a microtidal estuary. Reg. Stud. Mar. Sci., 59, doi: https://doi.org/10.1016/j.rsma.2022.102809

Gall, S. C., & Thompson, R. C., 2015. The impact of debris on marine life. Mar. Pollut. Bull., 92, 170-179, doi: https://doi.org/10.1016/j.marpolbul.2014.12.041

Hanvey, J. S., et al., 2017. A review of analytical techniques for quantifying microplastics in sediments. Anal. Methods, 9(9), 1369-1383, doi: https://doi.org/10.1039/C6AY02707E

Hervouet, J. M., 2007. Hydrodynamics of free surface flows: Modelling with the finite element method. John Wiley & Sons, doi: http://dx.doi.org/10.1002/9780470319628

Horton, A. A., Walton, A., Spurgeon, D. J., Lahive, E., & Svendsen, C., 2017. Microplastics in freshwater and terrestrial environments: evaluating the current understanding to identify the knowledge gaps and future research priorities. Sci. Total Environ., 586, 127-141, doi: https://doi.org/10.1016/j.scitotenv.2017.01.190

Ikenoue, T., Nakajima, R., Fujiwara, A., Onodera, J., Itoh, M., Toyoshima, J., ... & Kikuchi, T., 2023. Horizontal distribution of surface microplastic concentrations and water-column microplastic inventories in the Chukchi Sea, western Arctic Ocean. Sci. Total Environ., 855, 159564, doi: https://doi.org/10.1016/j.scitotenv.2022.159564

Isobe, A., Iwasaki, S., Uchida, K., & Tokai, T., 2019. Abundance of non-conservative microplastics in the upper ocean from 1957 to 2066. Nat. Commun., 10, Article 1-13, doi: https://doi.org/10.1038/s41467-019-08316-9

Jalón-Rojas, I., Wang, X., & Fredj, E., 2019. A 3D numerical model to track marine plastic debris (TrackMPD): Sensitivity of microplastic trajectories and fates to particle dynamical properties and physical processes. Mar. Pollut. Bull., 141, 256-272, doi: https://doi.org/10.1016/j.marpolbul.2019.02.052

Jalón-Rojas, I., Romero-Ramírez, A., Fauquembergue, K., Rossignol, L., Cachot, J., Sous, D., & Morin, B., 2022. Effects of biofilms and particle physical properties on the rising and settling velocities of microplastic fibers and sheets. Environ. Sci. Technol., 56(14), 8114-8123, doi: https://doi.org/10.1021/acs.est.2c01302

Jambeck, J. R., Geyer, R., Wilcox, C., Siegler, T. R., Perryman, M., Andrady, A., Narayan, R., & Law, K. L., 2015. Plastic waste inputs from land into the ocean. Science, 347(6223), 768-771, doi: https://doi.org /10.1126/science.1260352

Kaiser, D., Kowalski, N., & Waniek, J. J., 2017. Effects of biofouling on the sinking behavior of microplastics. Environ. Res. Lett., 12(12), doi: http://dx.doi.org/10.1088/1748-9326/aa8e8b

Kershaw, P. J., & Rochman, C. M., 2015. Sources, fate and effects of microplastics in the marine environment: Part 2 of a global assessment. Reports and Studies IMO/FAO/Unesco-IOC/WMO/IAEA/UN/UNEP Joint Group of Experts on the Scientific Aspects of Marine Environmental Protection (GESAMP).

Khatmullina, L., & Isachenko, I., 2017. Settling velocity of microplastic particles of regular shapes. Mar. Pollut. Bull., 114, 871-880, doi: https://doi.org/10.1016/j.marpolbul.2016.11.024

Kjerfve, B., 1986. Comparative oceanography of coastal lagoons. In D.A. Wolfe (Ed.), Estuarine Variability (pp. 63-81). Academic Press, doi: https://doi.org/10.1016/B978-0-12-761890-6.50009-5

Koelmans, A. A., Bakir, A., Burton, G. A., & Janssen, C. R., 2016. Microplastic as a vector for chemicals in the aquatic environment: Critical review and model-supported reinterpretation of empirical studies. Environ. Sci. Technol., 50(7), 3315-3326, doi: https://doi.org/10.1021/acs.est.5b06069

Lebreton, L. M., Greer, S. D., & Borrero, J. C., 2012. Numerical modelling of floating debris in the world's oceans. Mar. Pollut. Bull., 64(3), 653-661, doi: https://doi.org/10.1016/j.marpolbul.2011.10.027

Li, J., Liu, H., & Chen, J. P., 2018. Microplastics in freshwater systems: A review on occurrence, environmental effects, and methods for microplastics detection. Water Res., 137, 362-374, doi: https://doi.org/10.1016/j.watres.2017.12.056

Ling, S. D., Sinclair, M., Levi, C. J., Reeves, S. E., & Edgar, G. J., 2017. Ubiquity of microplastics in coastal seafloor sediments. Mar. Pollut. Bull., 121(1-2), 104-110, doi: https://doi.org/10.1016/j.marpolbul.2017.05.038

Lisboa, P. V., Fernandes, E. H., Sottolichio, A., Huybrechts, N., & Bendo, A. R., 2022. Coastal plumes contribution to the suspended sediment transport in the Southwest Atlantic inner continental shelf. Journal of Marine Systems, 236, 103796, doi: https://doi.org/10.1016/j.jmarsys.2022.103796

Lobelle, D., & Cunliffe, M., 2011. Early microbial biofilm formation on marine plastic debris. Mar. Pollut. Bull., 62(1), 197-200, doi: https://doi.org/10.1016/j.marpolbul.2010.10.013

Lobelle, D., Kooi, M., Koelmans, A. A., Laufkötter, C., Jongedijk, C. E., Kehl, C., & van Sebille, E., 2021. Global modeled sinking characteristics of biofouled microplastic. J. Geophys. Res. Oceans, 126(4), doi: https://doi.org/10.1029/2020JC017098

Meijer, L. J., Van Emmerik, T., Van Der Ent, R., Schmidt, C., & Lebreton, L.., 2021. More than 1000 rivers account for 80% of global riverine plastic emissions into the ocean. Sci. Adv., 7(23), doi: https://doi.org/10.1126/sciadv.aaz5803

Mitarai, S., Siegel, D. A., Watson, J. R., Dong, C., & McWilliams, J. C., 2009. Quantifying connectivity in the coastal ocean with application to the Southern California Bight. J. Geophys. Res. Oceans, 114, doi: https://doi.org/10.1029/2008JC005166

Möller, O. O., Castaing, P., Salomon, J. C., & Lazure, P., 2001. The influence of local and nonlocal forcing effects on the subtidal circulation of Patos Lagoon. Estuaries, 24(2), 297-311, doi: https://doi.org/10.2307/1352953

Moller Jr, O. O., Stech, J., & Mata, M. M., 1996. The Patos Lagoon summertime circulation and dynamics. Cont. Shelf Res., 16(3), 335-351, doi:

https://ui.adsabs.harvard.edu/link_gateway/1996CSR....16..335M/doi:10.1016/0278-4343(95)00014-R

Napper, I. E., & Thompson, R. C., 2019. Marine plastic pollution: Other than microplastic. Waste, 2, 425-442, doi: https://doi.org/10.1016/B978-0-12-815060-3.00022-0

Niencheski, L. F., Möller Jr, O. O., Odebrecht, C., & Fillmann, G., 1988. Distribuição espacial de alguns parâmetros físicos e químicos na Lagoa do Patos-Porto Alegre a Rio Grande, RS. Acta. Limnol. Bras., 11, 79-97.

Oliveira, H. A. D., Fernandes, E. H. L., Möller Junior, O. O., & Collares, G. L., 2015. Processos hidrológicos e hidrodinâmicos da Lagoa Mirim.

Paim, P. S., & Möller, O. O., 1986. Material em suspensão e dissolvido no estuário da Lagoa dos Patos–Fase III. Relatório Téc, FURG/CIRM.

Pan, Z., Guo, H., Chen, H., Wang, S., Sun, X., Zou, Q., ... & Huang, J., 2019. Microplastics in the Northwestern Pacific: Abundance, distribution, and characteristics. Sci. Total Environ., 650, 1913-1922, doi: https://doi.org/10.1016/j.scitotenv.2018.09.244

Pinheiro, L. M., Agostini, V. O., Lima, A. R. A., Ward, R. D., & Pinho, G. L. L., 2021. The fate of plastic litter within estuarine compartments: An overview of current knowledge for the transboundary issue to guide future assessments. Environ. Pollut., 279, 116908, doi: https://doi.org/10.1016/j.envpol.2021.116908

Pinheiro, L. M., Britz, L. M., Agostini, V. O., Pérez-Parada, A., García-Rodríguez, F., Galloway, T. S., & Pinho, G. L., 2022. Salt marshes as the final watershed fate for meso- and microplastic contamination: A case study from Southern Brazil. Sci. Total Environ., 838, 156077, doi: https://doi.org/10.1016/j.scitotenv.2022.156077

Santos, Í. E., Fernandes, E. H., Pinho, G. L., & Abdallah, P. R., 2023. Characteristics and fluxes of plastic debris based on socio-economic data for Patos Lagoon — A choked coastal lagoon in South Brazil. Environ. Sci. Pollut. Res., 30(44), 59382-59400, doi: https://doi.org/10.1007/s11356-023-26660-8

Shabaka, S., Moawad, M. N., Ibrahim, M. I., El-Sayed, A. A., Ghobashy, M. M., Hamouda, A. Z., ... & Youssef, N. A. E., 2022. Prevalence and risk assessment of microplastics in the Nile Delta estuaries: "The Plastic Nile" revisited. Sci. Total Environ., 852, 158446, doi: https://doi.org/10.1016/j.scitotenv.2022.158446

Silva, P. D., Fernandes, E. H., & Gonçalves, G. A., 2022. Sustainable Development of Coastal Areas: Port Expansion with Small Impacts on Estuarine Hydrodynamics and Sediment Transport Pattern. Water, 14, doi: https://doi.org/10.3390/w14203300

Silva, P. H., & de Sousa, F. D., 2021. Microplastic pollution of Patos Lagoon, south of Brazil. Environ. Challenges, 4, doi: http://dx.doi.org/10.1016/j.envc.2021.100076

Su, L., Xiong, X., Zhang, Y., Wu, C., Xu, X., Sun, C., & Shi, H., 2022. Global transportation of plastics and microplastics: A critical review of pathways and influences. Sci. Total Environ., 831, doi: https://doi.org/10.1016/j.scitotenv.2022.154884

Summers, E., Du, J., Park, K., & Kaiser, K., 2023. How does buoyancy behavior impact microplastic transport in an estuarine environment? Sci. Total Environ., 899, doi: https://doi.org/10.1016/j.scitotenv.2023.165687

Távora, J., Fernandes, E. H., Bitencourt, L. P., & Orozco, P. M. S., 2020. El-Niño Southern Oscillation (ENSO) effects on the variability of Patos Lagoon Suspended Particulate Matter. Reg. Stud. Mar. Sci., 40, Article 101495, doi: https://doi.org/10.1016/j.rsma.2020.101495

Távora, J., Fernandes, E. H., Thomas, A. C., Weatherbee, R., & Schettini, C. A., 2019. The influence of river discharge and wind on Patos Lagoon, Brazil, Suspended Particulate Matter. Int. J. Remote Sens., 40(11), 4506-4525, doi: http://dx.doi.org/10.1080/01431161.2019.1569279

Ranjani, M., Veerasingam, S., Venkatachalapathy, R., Jinoj, T. P. S., Guganathan, L., Mugilarasan, M., & Vethamony, P., 2022. Seasonal variation, polymer hazard risk and controlling factors of microplastics in beach sediments along the southeast coast of India. Environmental Pollution, 305, doi: https://doi.org/10.1016/j.envpol.2022.119315

Rodriguez, C., Silva, P., Marques, L., Lara, L., Fernandes, A., Bouyssou, R., ... & L Fernandes, E. L. 2024. Trajectory, Fate, and Magnitude of Continental Microplastic Loads to the Inner Shelf: A Case Study of the World's Largest Coastal Shallow Lagoon. Sci. Total Environ., 948, 174791, doi: https://doi.org/10.1016/j.scitotenv.2024.174791

Tsuchiya, M., Kitahashi, T., Nakajima, R., Oguri, K., Kawamura, K., Nakamura, A., ... & Fujikura, K., 2024. Distribution of microplastics in bathyal-to hadal-depth sediments and transport process along the deep-sea canyon and the Kuroshio Extension in the Northwest Pacific. Marine Pollution Bulletin, 199, 115466, doi: https://doi.org/10.1016/j.marpolbul.2023.115466

Vaz, A. C., Möller, O. O., & Almeida, T. L. D., 2006. Análise quantitativa da descarga dos rios afluentes da Lagoa dos Patos, doi: https://doi.org/10.5088/atl%C3%A2ntica.v28i1.1724

Waldschläger, K., & Schüttrumpf, H., 2019. Effects of particle properties on the settling and rise velocities of microplastics in freshwater under laboratory conditions. Environ. Sci. Technol., 53(4), 1958-1966, doi: https://doi.org/10.1021/acs.est.8b06794

Weinstein, J. E., Crocker, B. K., & Gray, A. D., 2016. From macroplastic to microplastic: Degradation of high-density polyethylene, polypropylene, and polystyrene in a salt marsh habitat. Environ. Toxicol. Chem., 35(7), 1632-1640, doi: https://doi.org/10.1002/etc.3432

Wright, S. L., Thompson, R. C., & Galloway, T. S., 2013. The physical impacts of microplastics on marine organisms: A review. Environ. Pollut., 178, 483-492, doi: https://doi.org/10.1016/j.envpol.2013.02.031

Zettler, E. R., Mincer, T. J., & Amaral-Zettler, L. A., 2013. Life in the “plastisphere”: Microbial communities on plastic marine debris. Environ. Sci. Technol., 47(13), 7137-7146, doi: https://doi.org/10.1021/es401288x